Crossover from anomalous to normal diffusion in porous media

F. D. A. Aarão Reis[1,*] and Dung di Caprio[2,†]

[1]*Instituto de Física, Universidade Federal Fluminense, Avenida Litorânea s/n, 24210-340 Niterói RJ, Brazil*
[2]*Institut de Recherche de Chimie Paris, CNRS, Chimie ParisTech, 11, rue P. et M. Curie, 75005 Paris, France*

Random walks (RW) of particles adsorbed in the internal walls of porous deposits produced by ballistic-type growth models are studied. The particles start at the external surface of the deposits and enter their pores in order to simulate an external flux of a species towards a porous solid. For short times, the walker concentration decays as a stretched exponential of the depth z, but a crossover to long-time normal diffusion is observed in most samples. The anomalous concentration profile remains at long times in very porous solids if the walker steps are restricted to nearest neighbors and is accompanied with subdiffusion features. These findings are correlated with a decay of the explored area with z. The study of RW of tracer particles left at the internal part of the solid rules out an interpretation by diffusion equations with position-dependent coefficients. A model of RW in a tube of decreasing cross section explains those results by showing long crossovers from an effective subdiffusion regime to an asymptotic normal diffusion. The crossover position and density are analytically calculated for a tube with area decreasing exponentially with z and show good agreement with numerical data. The anomalous decay of the concentration profile is interpreted as a templating effect of the tube shape on the total number of diffusing particles at each depth, while the volumetric concentration in the actually explored porous region may not have significant decay. These results may explain the anomalous diffusion of metal atoms in porous deposits observed in recent works. They also confirm the difficulty in interpreting experimental or computational data on anomalous transport reported in recent works, particularly if only the concentration profiles are measured.

I. INTRODUCTION

Diffusion in porous media long has been a topic of interest [1,2] due to a variety of technological applications, which are usually related to the large surface-to-volume ratio of those materials. The concentration profile of a diffusing species entering a disordered medium is typically of the form

$$\rho(z,t) \sim \exp\left[-z^\mu / R(t)\right], \tag{1}$$

where z is the direction perpendicular to the external surface, with $z = 0$ at that surface. The function $R(t)$ measures the spreading of the concentration profile in time t and asymptotically behaves as

$$R(t) \sim t^\alpha. \tag{2}$$

From Eqs. (1) and (2), the mean-square displacement of the diffusing material scales as

$$\langle z^2 \rangle \sim t^{2\alpha/\mu}. \tag{3}$$

Normal (Fickean) diffusion is characterized by a spatially Gaussian distribution of the diffusing species and linearly increasing mean-square displacement: $\mu = 2$ and $\alpha = 1$. Otherwise the diffusion is called anomalous. The scaling of $\langle z^2 \rangle$ is frequently used to separate cases of subdiffusion ($\alpha/\mu < 1/2$) and superdiffusion ($\alpha/\mu > 1/2$). The most frequently observed anomaly is subdiffusion because the irregularities of the porous media (e.g., barriers and dead ends) restrict the movement of the diffusing species.

The relevance of anomalous diffusion in real systems has been shown in several recent works. For instance, fluorescence spectroscopy was used to distinguish cases of normal and subdiffusion of tracer particles in colloidal crystals [3] and, combined with confocal microscopy (to probe concentration profiles), it was used to show that reaction-diffusion models were necessary to explain dye transport in metal-organic frameworks [4]. Nuclear magnetic resonance was recently used to measure exponents α and μ of water diffusion in several disordered colloidal systems, showing deviations from Fickean diffusion [5,6]. Particularly interesting cases of stretched exponential concentration profiles and superdiffusion were shown when Pt atoms entered the pores of porous carbon and anodic porous alumina during plasma sputtering deposition on those samples [7–9]. Moreover, due to the importance of subdiffusion phenomena in cells and model systems, the need for experimental standards was recently highlighted [10].

There is also an intense theoretical work on anomalous diffusion. Some approaches involve the computational study of fluid flow and solute transport in disordered media [11–16], analytical methods based on advection-diffusion equations [17,18], and fractional diffusion equations [19–22]. The study of random walks (RW) in models of disordered media [1,2] is another simple and widely used approach, whose relevance to describe real system features is illustrated in recent works [23–25].

Motivated by the observation of anomalous diffusion of Pt atoms penetrating samples of disordered porous carbon [7], in the first part of this work we study RW of particles adsorbed in the internal surface of porous deposits after being released at their outer surface. The deposits are produced by ballistic deposition (BD) [26,27] and by an extension of that model [28–31]. For short times, the concentration profiles are stretched exponentials [slower than Gaussian, $\mu < 2$ in Eq. (1)]. This feature is still observed at long times in one type of deposit, and the corresponding time scaling

*reis@if.uff.br
†dung.dicaprio@yahoo.fr

of the concentration profile is consistent with subdiffusion. The area explored by the walkers decreased approximately as the inverse of the depth in this case. Tracer particles inside the samples do not show dependence of diffusion coefficients on the depth, which rules out theoretical approaches with this assumption. Although the values of exponents μ and α differ from those of Ref. [7], the scaling of the concentration with depth and time show similar deviations from normal diffusion.

The second part of this work is devoted to the study of random walks in tubes of decreasing cross section, which show concentration profiles with stretched exponentials and anomalous scaling of the mean-square displacement. A tube with area decreasing with the inverse of the depth (similarly to the porous deposits with anomalous diffusion) shows significant deviations from normal scaling and exponent values much closer to those of Pt atoms entering porous carbon samples [7]. A detailed discussion of the crossover from anomalous to normal diffusion is presented for the case of tubes with exponentially decreasing cross section, in which analytical solution is possible. These results confirm the difficulty in interpreting experimental or computational data on anomalous transport, particularly the concentration profiles, consistently with recent works [3,10,25,32].

This paper is organized as follows. In Sec. II, we present the models of ballistic deposits and the random-walk models. In Sec. III, we study the scaling of concentration profiles inside the ballistic deposits and related quantities. In Sec. IV, we study diffusion in tubes of decreasing cross section and discuss the crossover in concentration scaling. In Sec. V, our conclusions are presented.

II. POROUS DEPOSITS AND RANDOM-WALK SIMULATION

Here we describe the two types of disordered porous media used in this work and the two types of RW simulated inside those samples.

In the BD model, particles are released from a randomly chosen position above a d-dimensional substrate, follow trajectories perpendicular to an initially flat substrate [here a (x,y) plane], and stick upon the first contact with a nearest neighbor (NN) occupied site, which may be the substrate or a previously deposited particle [26,27]. The aggregation rules are illustrated in Fig. 1(a). The resulting aggregate is porous and has a rough surface, as illustrated in the cross-sectional view of a three-dimensional deposit in Fig. 1(b). Long-time simulations indicate that the porosity is approximately 0.667.

A simple extension of that model, called BDNNN, allows aggregation of the incident particle by contact with a NN or a next-nearest-neighbor (NNN) occupied site [28–31], as illustrated in Fig. 1(c). The resulting deposit has a larger porosity, approximately 0.834, as illustrated by the cross-sectional view of Fig. 1(d) with an identical number of deposited layers as in Fig. 1(c).

Deposits of average heights near 900 lattice units and lateral sizes 1024 were grown. The structure of each sample remains fixed during the simulation of diffusion, i.e., they are nondeformable porous solids. A single deposit is large enough to represent all the microscopic environments that are relevant for the RW statistics. For this reason, only three samples were
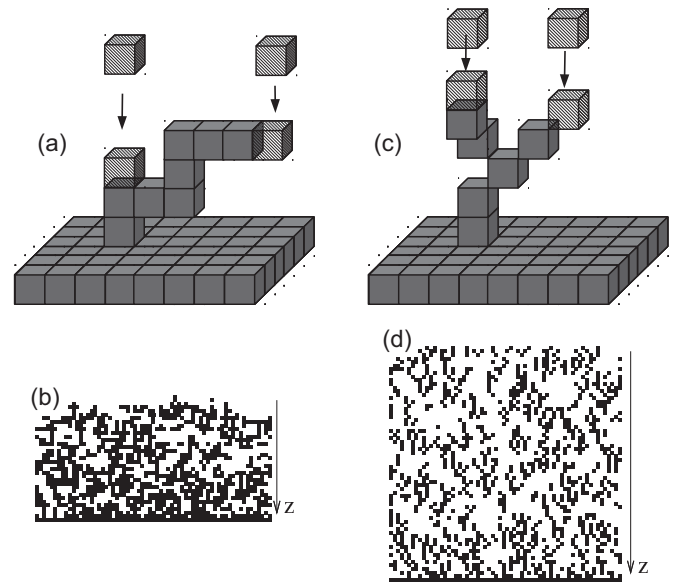

FIG. 1. Illustration of the aggregation rules and cross sections of the tops of deposits generated by [(a) and (b)] BD and [(c) and (d)] BDNNN. Dark gray cubes are previously aggregated solid particles and light gray cubes are incident particles, whose aggregation positions (also shown in light gray) are indicated by arrows.

produced by each growth model (BD and BDNNN) and used in RW simulations, providing approximately the same average quantities; for instance, the dispersion in the porosity is smaller than 0.3%.

The maximal height of a solid particle in each column (x,y) of a deposit is defined as the column height $h(x,y)$. The set $\{h(x,y)\}$ defines the external surface of the deposit. The average $\bar{h}$ of that set is taken as the position $z = 0$ for RW simulations. The z axis is oriented to the interior of the deposit, perpendicularly to the substrate where it was grown. This is illustrated in Figs. 1(b) and 1(d).

In each porous sample, 2^{25} ($\sim 10^8$) noninteracting walkers are left at $t = 0$ at randomly chosen points with $z = 0$, with the condition that at least one NN of the starting point is a solid site. In one time unit, one step trial is performed for each walker. Adsorption to the porous solid is always required, i.e., only steps to points that also have a NN solid site are allowed.

Independent simulations were performed with two possible conditions for choosing the steps of the walkers: (I) a step to a NN site of the underlying cubic lattice (6 possibilities) is randomly chosen and (II) a step to a NN or a NNN site of the underlying cubic lattice (18 possibilities) is randomly chosen. If the target site has at least one NN of the porous solid (adsorption condition), then the step is executed. Otherwise the step trial is rejected and the walker remains at the same position.

Figures 2(a) and 2(b) illustrate steps with conditions (I) and (II), respectively. Diffusion under condition (I) is severely restricted because it does not allow corner rounding. However, with condition (II), this process is possible and steps from one branch of the porous solid to another one are facilitated.

The maximum simulation time is 10^5, corresponding to the maximum number of possible steps of each walker (due to the no-desorption condition, the number of executed steps may
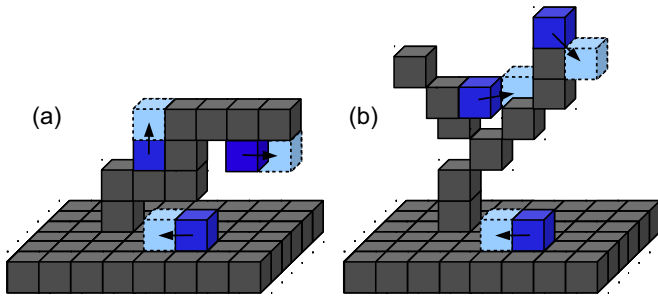
FIG. 2. (Color online) Illustration of possible steps of RW of the species (dark blue) moving inside the porous medium (solid part in dark gray) according to rules (a) (I) and (b) (II). The target position of the allowed steps is shown in light blue.

be much smaller than that). This maximal time is suitable to avoid that any walker reaches the bottom of the substrate.

As a final remark, we recall that there are other extensions of BD to represent a variety of porous materials [33–38]. However, the aim of this work is to understand basic features of anomalous diffusion of a species entering a porous material, instead of representing a particular application. For this reason, we restrict our work to the study of samples produced by BD and BDNNN models.

III. DIFFUSION IN THE POROUS DEPOSITS

A. Scaling of concentration profiles

Figures 3(a) and 4(a) show $\log[-\log(\rho/\rho_0)]$ as a function of $\log z$ in three different times for RW in porous solids produced by BD [lower porosity, Fig. 1(b)], respectively, with conditions (I) and (II) for the steps. Here ρ_0 is the maximum value of the density profile. Figures 5(a) and 6(a) show the same quantities for RW in porous solids produced by BDNNN [high porosity, Fig. 1(d)], respectively, with conditions (I) and (II) for the steps.

Linear fits of the data for large z are also shown in Figs. 3(a), 4(a), 5(a), and 6(a). Their slopes are estimates of the exponent μ in Eq. (1). At short times ($t = 10^3$), the slopes are significantly below 2 in all cases. This is usually a transient behavior, since the fits of the data at longer times ($t = 10^4$ and $t = 10^5$) in Figs. 3(a), 4(a), and 6(a) have slopes close to the normal diffusion value $\mu = 2$ (deviations are smaller than 10%). However, in BDNNN deposits, the stretched concentration decay (slower than Gaussian) is observed up to very long times, with fits in Fig. 5(a) ranging from $\mu \approx 1.33$ to $\mu \approx 1.40$ in depths ranging from $z \sim 1$ to $z \approx 250$ (in units of the lattice constant).

The plots of the concentration profiles are rescaled by the time t in Figs. 3(b), 4(b), 5(b), and 6(b). Reasonable data
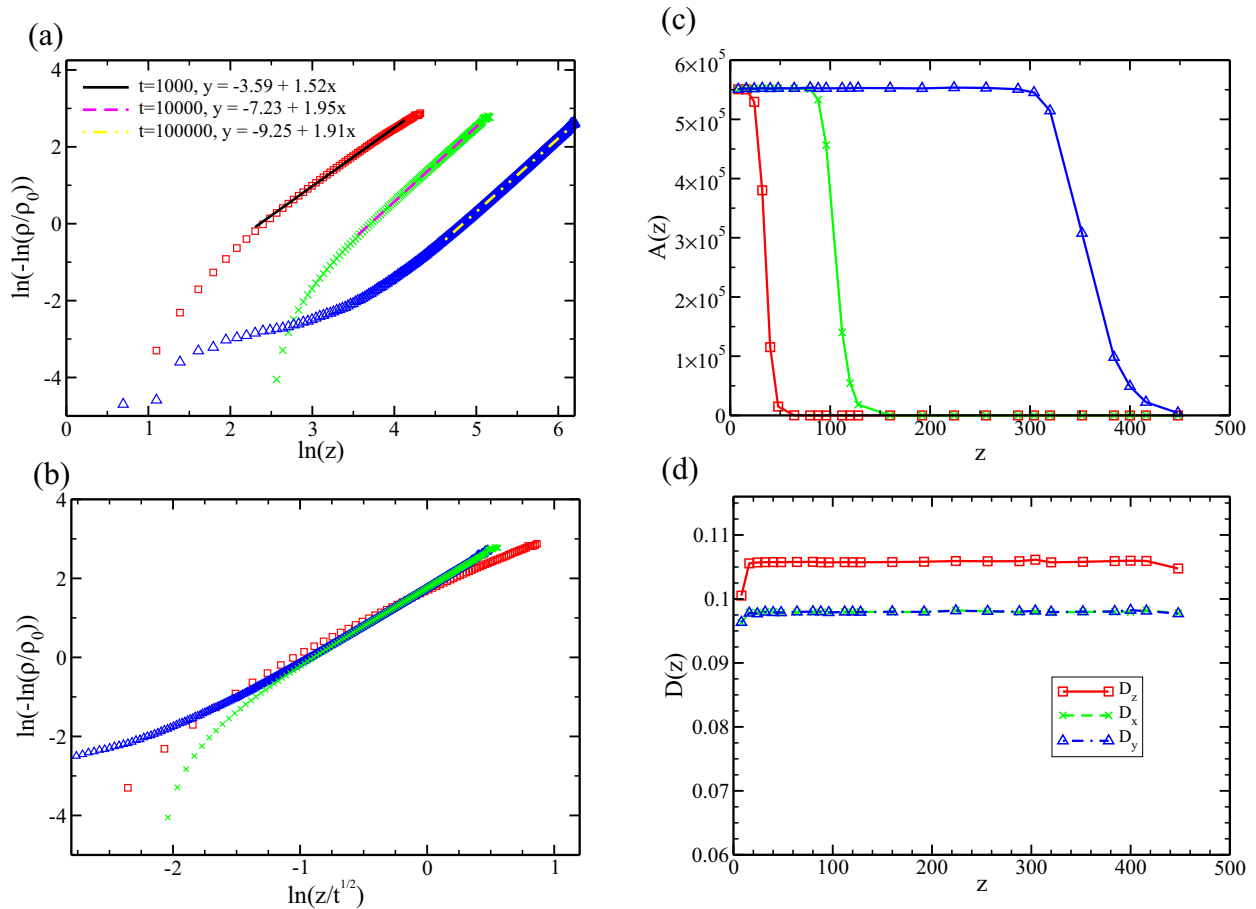

FIG. 3. (Color online) Concentration profiles without (a) and with (b) time scaling, number of sites explored by RW (c), and local diffusion coefficients (d) of tracer particles as a function of the depth z in porous solids produced by BD with rule (I) for the random steps of the RW. In (a), (b), and (c), red squares, green crosses, and blue triangles relate respectively to $t = 1000$, 10 000, 100 000. Full, dashed, and dash-dot-dot lines in (a) are linear fits for the largest values of z.
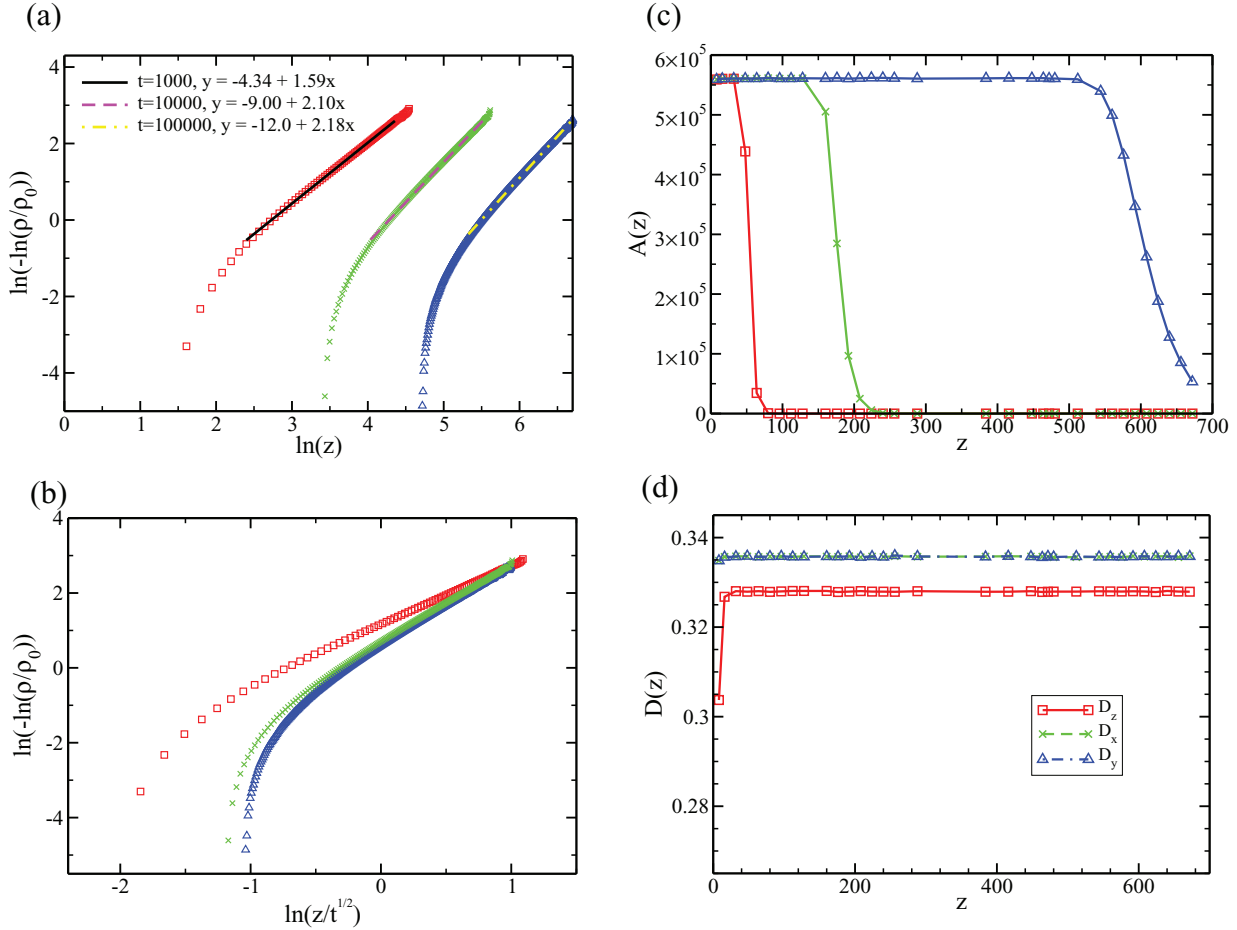
FIG. 4. (Color online) Concentration profiles without (a) and with (b) time scaling, number of sites explored by RW (c), and local diffusion coefficients (d) of tracer particles as a function of the depth z in porous solids produced by BD with rule (II) for the random steps of the RW. Points and lines are as defined in the caption to Fig. 3.

collapse of the large z data is obtained in Figs. 3(b), 4(b), and 6(b), using the scaling variable $z/t^{1/2}$, which gives $\alpha/\mu = 1/2$ [Eqs. (1) and (2)]. This is consistent with asymptotic normal diffusion.

On the other hand, walkers of type (I) in BDNNN deposits show much slower time dependence of the concentration profile, which could be anticipated by comparison of Fig. 5(a) with Figs. 3(a), 4(a), or 6(a). A reasonable data collapse for large z is obtained in Fig. 5(b) with the scaling variable $z/t^{0.15}$, which gives $\alpha/\mu \approx 0.15$ [Eqs. (1) and (2)]. This estimate gives $\langle z^2 \rangle \sim t^{0.3}$, which indicates subdiffusion. A comparison with experimental results is interesting at this point.

For Pt atoms entering porous carbon samples, Ref. [7] gives $\mu \approx 0.55$, which characterizes a stretched decay (much slower than Gaussian) of the concentration profile and gives a very slowly increasing $R(t)$, with $\alpha \approx 0.2$. Combination of these results gives $\langle z^2 \rangle \sim t^{0.72}$, i.e., $\alpha/\mu = 0.36$ [Eqs. (1) and (2)]. In the usual classification [1,2], a system with $\alpha/\mu < 1/2$ is a case of subdiffusion (however, the remarkable stretching of the concentration profile is a nontrivial feature that led the authors of Ref. [7] to propose it was superdiffusive scaling).

For water diffusion in disordered colloidal systems, Ref. [5] shows that several combinations of $\alpha < 1$ and $\mu < 2$ are possible, which may give sub- or superdiffusion. However, in that case, all estimates are close to $\alpha = 1$ and $\mu = 2$.

A recent work on Pt atoms entering pores of anodic alumina [9] reported $\mu \approx 1/3$ and $\alpha \approx 1.25$, which gives a remarkably rapid superdiffusion [$2\alpha/\mu \approx 7.5$; Eq. (3)]. However, the organized geometry of those samples make them differ markedly from our deposits.

Finally, we recall that subdiffusion was also observed in porous deposits produced by other ballistic-like models in Ref. [23]. Those deposits seem to have lower porosity than ours and have different pore shapes and connectivity. Only the mean-square displacement of the walkers was studied in that work, thus the present results strongly suggest the study of concentration profiles in those samples.

B. Explored area and diffusion coefficients

The anomalous diffusion for walkers of type (I) in BDNNN deposits is related to several constraints for their steps, similarly to other systems [2]. First, the volume accessible for the walkers is restricted because the porosity is very large [Fig. 1(d)] and they are always adsorbed to the internal solid walls. Second, since the steps are restricted to NN [Fig. 2(a)], some movements become impossible, such as the corner rounding shown for the upper walker in Fig. 2(b). This is certainly an important contribution to anomalous scaling.
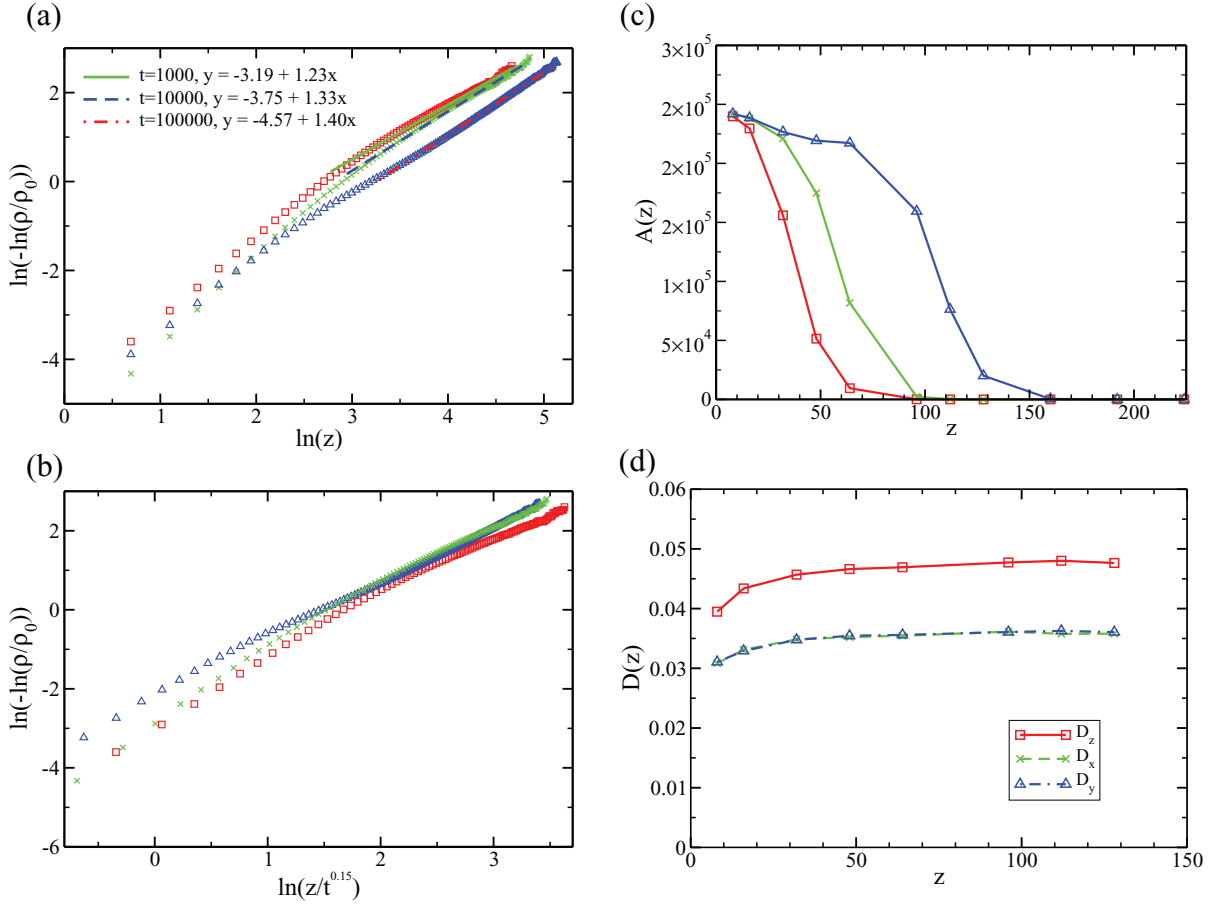
FIG. 5. (Color online) Concentration profiles without (a) and with (b) time scaling, number of sites explored by RW (c), and local diffusion coefficients (d) of tracer particles as a function of the depth z in porous solids produced by BDNNN with rule (I) for the random steps of the RW. Points and lines are as defined in the caption to Fig. 3.

Here we measure some quantities that help to explain the results presented in Sec. III A and motivate the models presented in Sec. IV.

The pore region accessible for the walkers is characterized by the total area $A(z)$ explored by the walkers at each depth z, for several times. This area is the total number of pore sites at depth z that have been occupied by a walker at least once up to time t. The explored areas $A(z)$ for three different times are shown in Figs. 3(c), 4(c), 5(c), and 6(c), for the respective solids and step conditions.

The three cases with transient anomalous scaling (Figs. 3, 4, and 6) show similar behavior of $A(z)$ for short and long times. For short times ($t \lesssim 1000$), there is a rapid decay of $A(z)$ at depths varying from ≈ 40 to ≈ 100, depending on the type of solid and the allowed steps. The corresponding fits of the concentration profiles extend to larger depths and show anomalous scaling ($\mu < 2$). For long times, the flat region of $A(z)$ extends to much larger depths, which means that the walkers explore an approximately constant cross section as they penetrate in the porous deposits. The corresponding concentration profiles show normal scaling $\mu = 2$.

For walkers of type (I) in BDNNN deposits, Fig. 5(c) shows a slow decay of $A(z)$ until very long times. A fit of the data in Fig. 5(c) for $t = 10^5$ suggests an approximate decay as

$A(z) \sim 1/z$. Thus, there is an actual reduction of the area that can be reached by the walkers as they penetrate in the porous solid. The porosity is approximately depth independent, which means that a large part of the porous space is not accessible to particles moving with the constraint of adsorption to the internal walls.

Figures 7(a)–7(d) show cross sections of a BDNNN solid at four depths z and highlights the area occupied by walkers of type (I) at $t = 10^5$. It confirms the reduction of the explored area with the depth. As will be shown in Sec. IV, the stretched decays of concentration profiles is intimately related to this feature.

Many works on anomalous diffusion connect this feature to position-dependent diffusion coefficients (see, e.g., Refs. [21,39]). In the present systems, this possibility is ruled out by measuring local diffusion coefficients that characterize the diffusion process in a narrow range around each depth z (in opposition to asymptotic coefficients that would characterize the diffusion in the full pore network).

The local diffusion coefficient at height z is measured by tracers left at all accessible points in the corresponding depth of the solid. The number of tracers left at each point (x,y,z) is proportional to the number of walkers which have occupied that position in the course of the original simulations up to $t = 10^5$ (i.e., in the simulations with walkers left at the external
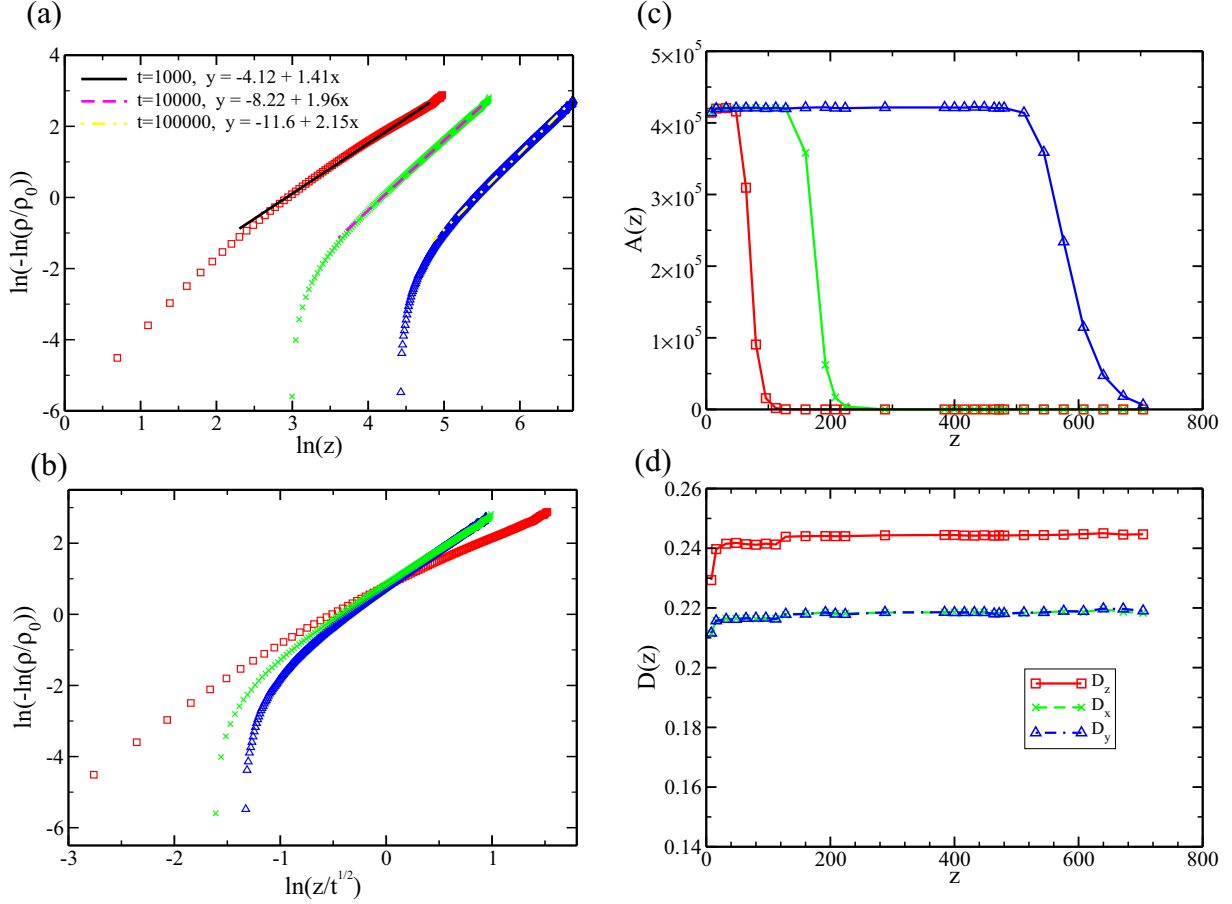
FIG. 6. (Color online) Concentration profiles without (a) and with (b) time scaling, number of sites explored by RW (c), and local diffusion coefficients (d) of tracer particles as a function of the depth z in porous solids produced by BDNNN with rule (II) for the random steps of the RW. Points and lines are as defined in the caption to Fig. 3.

surface). Each tracer tries to execute a small number of steps, $t_0 = 100$, following the same rules [(I) or (II)] of the RW. For the set of tracers starting at a given depth z', the mean-square vertical displacement $\langle (\Delta z)^2 \rangle (z', t_0)$ is measured after t_0 steps (averaging over x, y, and different tracers). The resulting local diffusion coefficient at depth z' is estimated as

$$D_z(z') = \frac{\langle (\Delta z)^2 \rangle (z', t_0)}{t_0}. \qquad (4)$$

$D_x(z')$ and $D_y(z')$ are equivalently measured.

Figures 3(d), 4(d), 5(d), and 6(d) show $D_z(z)$ as a function of the depth z, for the respective solids and walker types of Figs. 3–6. Considering the small values of the diffusion coefficients, we observe that only a small region around the original position is explored, thus we are actually measuring local diffusion coefficients. In all cases, the coefficients are approximately depth independent, which means that the porous solids are homogeneous at short length scales. Thus, the anomalous diffusion observed in these systems cannot be explained by changes in the local diffusion coefficient. This contrasts to some widely used models of anomalous diffusion [21,39] and the proposed generalized diffusion equation of Ref. [7].

Figures 3(d), 4(d), 5(d), and 6(d) also show the diffusion coefficients $D_x(z)$ and $D_y(z)$, with no significant dependence on z. The estimates of $D_x(z)$ and $D_y(z)$ are nearly the same,

which confirms the homogeneity in the horizontal directions and the accuracy of the simulations.

We conclude that local features of the porous deposits are not responsible for the anomalous diffusion observed here. Instead, the anomaly is related to the different accessibility of inner sites at a given height, since they have different connections (if any) to the outer surface.

IV. DIFFUSION IN TUBES OF VARIABLE CROSS SECTION

The work with RW entering porous deposits showed anomalous diffusion when the available area for the walkers decreased with the depth but with constant diffusion coefficients. For this reason, this second part of the paper considers a simple model with those features.

A. Basic equations and crossover

We consider an ensemble of RW starting at randomly chosen positions with $z = 0$ at $t = 0$, confined to move in the three-dimensional region $z \geqslant 0$, $x^2 + y^2 \geqslant [A(z)/\pi]$, which defines a tube of z-dependent cross section $A(z)$. Here we are interested in cases where $A(z)$ is monotonically decreasing, similarly to the porous media produced by BDNNN. An illustration is provided in Fig. 8(a).
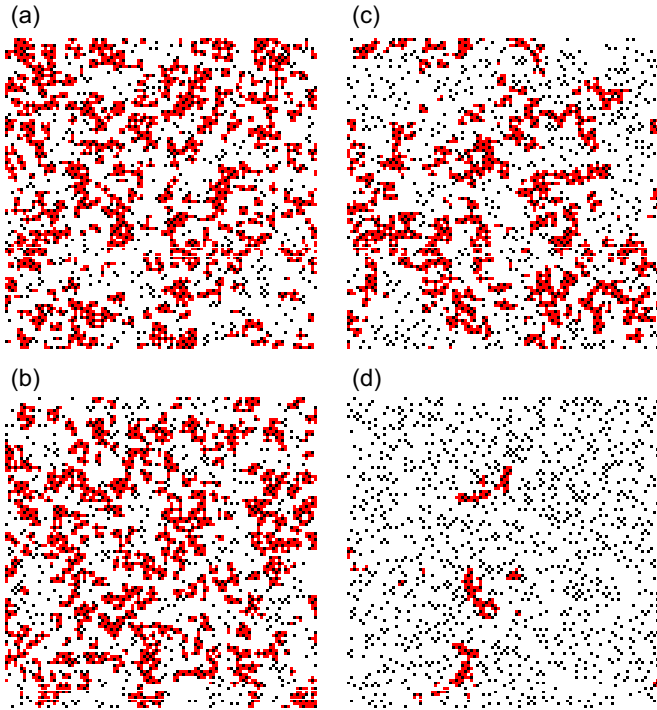
FIG. 7. (Color online) Cross sections of a porous solid produced by BDNNN at depths (a) $z = 16$, (b) 32, (c) 96, and (d) 128, with solid part in black, porous sites visited by RW [rule (I)] at $t = 10^5$ in red and nonvisited porous part in white.

Let $N(z,t)$ be the number of walkers at position z at time t. This quantity is proportional to the walker concentration $\rho(z,t)$ if the latter is measured over a constant cross section, i.e., the cross section of a solid containing the empty tube. This is similar to the measurement of concentration in the porous deposits of Sec. III A and in experimental works, since the total number of walkers at each depth z is divided by the (constant) area of a slice that includes solid parts and pores.

In the limit of continuous z and t, the change in $N(z,t)$ in a small time interval is

$$N(z,t + \Delta t) - N(z,t)$$
$$= -kN(z,t) + kN(z - \Delta z,t)\frac{A(z)}{A(z - 2\Delta z) + A(z)}$$
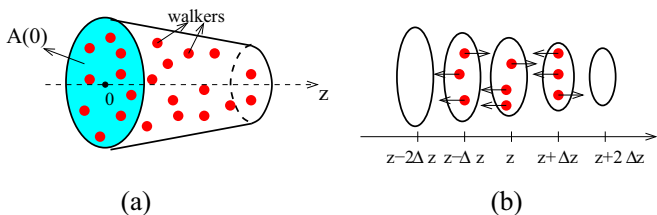$$+ kN(z + \Delta z,t)\frac{A(z)}{A(z + 2\Delta z) + A(z)}, \quad (5)$$

FIG. 8. (Color online) (a) Tube with z-dependent cross section and walkers moving inside it; (b) random steps of the walkers in the tube, with larger number of steps towards the larger neighboring areas.

where k is a constant (increasing with Δt and decreasing with Δz). Equation (5) accounts for the fact that all neighboring sites are equally probable for a random step, thus the number of walkers that move from $z \pm \Delta z$ to a neighboring position ($z \pm 2\Delta z$ or z) is proportional to the area available at that position. This is illustrated in Fig. 8(b), with a larger number of walkers moving to the larger neighboring area.

Considering that $A(z \pm 2\Delta z) + A(z) \approx 2A(z \pm \Delta z)$ and dividing Eq. (5) by $A(z)$, we obtain an equation for $N(z,t)/A(z)$. Defining $D \equiv k\Delta z^2/\Delta t$ and taking the continuum limit ($\Delta z \rightarrow 0$, $\Delta t \rightarrow 0$), we obtain

$$\frac{\partial(N/A)}{\partial t} = \frac{D}{2}\frac{\partial^2(N/A)}{\partial z^2}. \quad (6)$$

This is the usual diffusion equation for the density $N(z,t)/A(z)$.

The solution of Eq. (6) is

$$N(z,t) = N_0 A(z) \exp[-z^2/(2Dt)], \quad (7)$$

where N_0 is a normalization constant dependent on t (typically as a power law, which is slowly varying compared to the exponential factor); for instance, for constant A, the normal value $N_0 A = \frac{1}{\sqrt{2Dt}}$ is recovered. This solution for $N(z,t)$ is a normal diffusion behavior with the concentration at position z templated by the area of the tube.

Rewriting the walker concentration of Eq. (7) as

$$N \sim \exp[-z^2/(2Dt) + \ln A(z)], \quad (8)$$

a crossover is expected if $|\ln A(z)|$ does not scale as z^2, i.e., non-Gaussian $A(z)$. Here we restrict the discussion to the cases in which $A(z)$ decreases slower than a Gaussian. In these cases, the first term in the exponential of Eq. (8) is dominant for large z, but the second one is larger for small z, particularly for long times. A crossover position z_c is found by matching the two terms in the exponential of Eq. (8), which gives

$$z_c^2/(2Dt) \approx \ln A(z_c). \quad (9)$$

Normal diffusion concentration is observed for $z \gg z_c$ and anomalous diffusion is observed for $z \ll z_c$, with a stretched exponential decay (slower than Gaussian) of the concentration profile.

As time increases, z_c increases, so the anomalous diffusion regime extends to larger regions and to lower densities. In this regime, matching the dominant terms of Eqs. (1) and (7), the anomaly exponent is given by power counting in the relation $\ln A(z) \sim z^\mu$.

Normal diffusion is able to distribute a large particle density in domains of size

$$z_{\text{diff}} \sim \sqrt{Dt}, \quad (10)$$

thus this is a region far from the Gaussian tail of the concentration profile. If diffusion takes place in a physically confined region, then the particle density (taken over porous and solid regions) is templated by the shape of the confined pore space up to $z \approx z_{\text{diff}}$. In other words, the concentration profile scales similarly to $A(z)$ in this highly populated region. Consequently, it is the templating effect of the tube shape that leads to a concentration decay similar to $A(z)$ for small z and the crossover phenomenon described above.
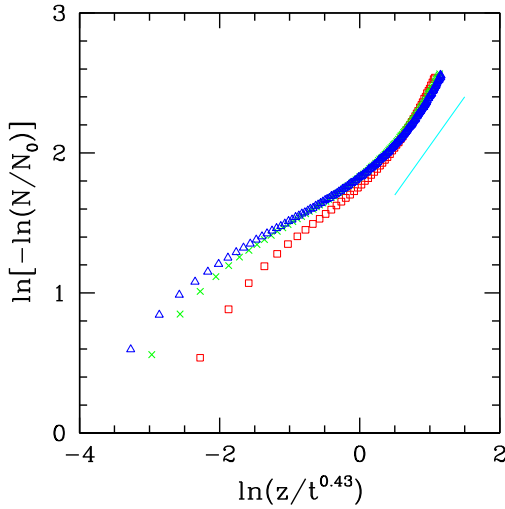
FIG. 9. (Color online) Normalized walker concentration as a function of the scaled depth in a tube with $A(z) = A_0/z$ at $t = 1000$ (red squares), $t = 5000$ (green crosses), and $t = 10\,000$ (blue triangles) and the solid line has slope 0.7.

B. Tubes with $A(z) \sim A_0/z$

As a first numerical application, we consider a tube with $A(z) = A_0/z$, where $A_0 = 10^4$. This is a decay similar to the explored area of RW of type (I) in BDNNN deposits (Sec. III). Simulations of 10^8 different walks were performed. In each walk, the particle executes one random step to a NN site per time unit, thus $D = 1/3$ in Eq. (6). Equation (7) gives $N \sim \frac{A_0}{z} \exp[-z^2/(2Dt)]$.

In Fig. 9, the usual scaling plot of the concentration profile is shown. The scaling variable $z/t^{0.43}$ provides the best fit for large z, where the slope is near 0.7, which is much smaller than the normal diffusion exponent $\mu = 2$. That estimate is obtained in a narrow region of the scaling variable, thus it may not be viewed as a true scaling exponent. However, taking it as an effective estimate of μ and taking $\alpha \approx 0.43$ (from the scaling variable in Fig. 9), we obtain $\langle z^2 \rangle \sim t^{0.86}$ [Eqs. (1) and (2)]. This corresponds to an apparent subdiffusion.

These results and those for walkers of type (I) in BDNNN deposits show important similarities. Both systems have stretched exponential decay of the concentration profile, a feature that is enhanced in the tube. They also show slowly increasing (subdiffusive) mean-square displacement, this effect being enhanced in the porous deposits. The slopes of scaling plots differ due to the different microscopic structures.

Surprisingly, the effective exponents obtained from Fig. 9 ($\mu \approx 0.7$, $\alpha \approx 0.3$) are much closer to the ones for Pt atoms entering porous carbon samples ($\mu \approx 0.55$ and $\alpha \approx 0.2$) [7], with the particularly interesting feature of highly stretched concentration profile. This suggests that the anomalous scaling observed in Pt atom diffusion may be a consequence of a very long crossover due to the confined geometry of those samples.

C. Tubes with exponentially decreasing cross section

Here we consider the case of exponential decay of $A(z)$ because this facilitates the analytical study of crossover effects,

$$A(z) = A_0 \exp(-z/z_0). \tag{11}$$

This gives $N(z,t) = N_1 \exp[-z^2/(2Dt) - z/z_0]$, where N_1 depends on A_0, z_0, and t [N_1 should not be confused with N_0 in Eq. (7): $N_0 = N_1 \exp(-z/z_0)$]. The crossover position is

$$z_c \approx 2Dt/z_0 \tag{12}$$

and the concentration relative to the origin at the crossover region is

$$\rho_c \equiv N(z_c,t)/N(0,t) \sim \exp(-4Dt/z_0^2). \tag{13}$$

For $z \gg z_c$, the asymptotically normal diffusion is observed, with density $\rho \ll \rho_c$. This corresponds to very small concentrations at long times, thus this regime is difficult to observe in simulation or in possible experimental realizations. For $z \ll z_c$, $N(z,t)$ follows the simple exponential decay of $A(z)$, which is the templating effect of the tube shape. The diffusion seems to be anomalous, with $\mu \approx 1$, and the concentration is much larger than ρ_c. As time increases, this regime extends to larger distances and lower densities.

The mean-square displacement $\langle z^2(t) \rangle \sim \int_0^\infty z^2 \rho(z,t)dz$ is estimated by finding the maximal value of $z^2 \rho(z,t)$, which occurs for $z = z_{\max} = [\sqrt{Dt/z_0^2 + 8} - \sqrt{Dt}/z_0]\sqrt{Dt}/2$. For $z_0 \gg \sqrt{Dt} \sim z_{\mathrm{diff}}$ [Eq. (10)], normal scaling with $\langle z^2 \rangle \sim t$ is obtained. This is a case in which the tube does not template the concentration profile. For $z_0 \ll \sqrt{Dt} \sim z_{\mathrm{diff}}$, $\langle z^2 \rangle \approx z_0^2$, with corrections in $1/t$, since the concentration profile follows the tube shape [$\rho \sim A(z)$ in the region contributing to $\langle z^2 \rangle$]. This is a case of anomalously slow diffusion ($\alpha = 0$). These limiting behaviors indicate that subdiffusion is expected in the crossover region.

The crossover is illustrated in Fig. 10(a) for a tube with $z_0 = 20$ at three different times. The distributions were obtained in simulations of 10^7 different walks with $D = 1/3$. For $t = 10^3$, a crossover is observed from an initial regime with slope ≈ 0.6 to a final regime with slope near 2. Again, we stress that these values are effective exponents representative only of a narrow scaling region. Equation (12) predicts the crossover length $z_c \approx 33$ for $z_0 = 20$ and $t = 10^3$, in good agreement with the results in Fig. 10(a). For $t = 10^5$, Fig. 10(a) does not show any signature of a crossover up to $z \approx 180$, which is the maximal depth in which accurate concentrations could be estimated. Moreover, the data in Fig. 10(a) do not fit a single scaling curve with any variable of the form $z/t^{\alpha/\mu}$.

An illustration of the crossover scaling is possible in tubes with $z_0 = 50$ and a smaller time range. Figure 10(b) shows $\ln[-\ln(N/N_0)]$ as a function of $\ln z/t^{0.43}$ at $t = 1000$, $t = 5000$, and $t = 10\,000$. The traditional form of the scaling variable gives a reasonable data collapse for large z in this system and indicates an effective anomalous diffusion (note that a complete scaling plot in this problem would have to involve the crossover length z_c). The initial slope is near 0.6 and crosses over to a slope near 1.7 for the largest values of z. These values are close to the predictions of effective exponents 1 and 2 of the crossover scaling; deviations are justified by the limited range of z in which the concentration is not negligible. The crossover positions predicted by Eq. (9) range from $z_c \approx 13$ ($t = 1000$) to $z_c \approx 130$ ($t = 10000$), which are close to the points with largest curvatures in the plots of Fig. 10(b).
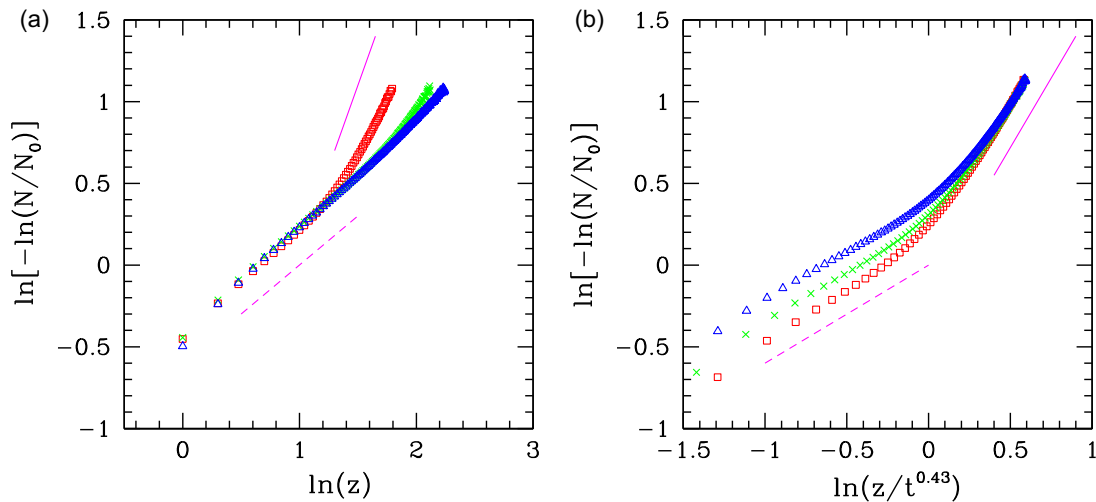
FIG. 10. (Color online) (a) Normalized walker concentration as a function of the depth in a tube with exponentially decreasing $A(z)$ with $z_0 = 20$ at $t = 1000$ (red squares), $t = 10\,000$ (green crosses), and $t = 100\,000$ (blue triangles). The dashed line has slope 0.6 and the solid line has slope 2. (b) Normalized walker concentration as a function of the scaled depth in a tube with exponentially decreasing $A(z)$ with $z_0 = 50$ at $t = 1000$ (red squares), $t = 2000$ (green crosses), and $t = 5000$ (blue triangles). The dashed line has slope 0.6 and the solid line has slope 1.7.

V. CONCLUSION

In the first part of this work, we studied the statistics of RW starting at the outer surface of porous deposits and restricted to move along their internal walls. The BD and BDNNN models were used to produce the porous solids. These conditions are chosen to parallel the penetration of metal atoms in porous materials during the deposition of a film at their external surfaces. The concentration decay with the depth z is slower than Gaussian at short times. At long times, a change to normal diffusion is observed in most cases. However, the stretched exponential concentration profile remains in the most porous solids, produced by BDNNN, if the walker steps are restricted to nearest neighbors. This feature is correlated to a decay of the area explored by the RW approximately with the inverse z. However, RW of tracer particles left at various points of the solid do not show a significant dependence of the diffusion coefficient with z. This rules out the description of the anomalous diffusion by equations with position-dependent coefficients [21,39]. This shows that local features in space or time are not of main importance for the anomaly, but the global history in the penetration of the diffusing particles is the main ingredient. Starting from surface deposition sites, not all inner sites at a given height are accessible in an equivalent way, some sites having a preferential path connecting them to the outer surface.

In the second part of the work, we propose a model of RW confined to a tube of decreasing cross section $A(z)$. We first consider an area which decreases slower than a Gaussian, similar to the decay obtained in one of the simulated experiment of the first part and account for a subdiffusion regime. Then considering the specific case of $A(z)$ with a simple exponential decay, we predict analytically the crossover from a subdiffusion to a normal diffusion regime. The crossover position and crossover density show good agreement with numerical data. In both cases, the anomalous scaling is understood as a templating effect of $A(z)$ on the concentration profile, which is measured in solid slices of constant area but with walkers exploring only a fraction of this area.

The above results suggest an alternative explanation to the stretched exponential concentration profiles and anomalous diffusion shown in recent works on the penetration of Pt atoms in disordered porous deposits [7], despite the difference in the exponent values. An interesting feature of our models is the independence of diffusion coefficients on the position, which is related to the local homogeneity of the media, while the model equations used in Ref. [7,9] assume a dependence of those coefficients in time and position. On the other hand, those experiments also include a flux of atoms to the outer surface of the porous media, which is a feature not included in the present models and certainly important for their quantitative description.

Independently of this possible application, the present work highlights the difficulty in interpreting experimental or computational data on anomalous diffusion, particularly if only the concentration profiles are measured or large crossover times are present. This is in agreement with recent experimental and theoretical works on the subject [3,10,25,32].

[1] J. P. Bouchaud and A. Georges, Phys. Rep. **185**, 127 (1990).

[2] S. Havlin and D. Ben-Avraham, Adv. Phys. **36**, 695 (1987).

[3] R. Raccis, A. Nikoubashman, M. Retsch, U. Jonas, K. Koynov, H.-J. Butt, C. N. Likos, and G. Fytas, ACS Nano **5**, 4607 (2011).

[4] S. Han, T. M. Hermans, P. E. Fuller, Y. Wei, and B. A. Grzybowski, Angew. Chem. Int. Ed. **51**, 2662 (2012).

[5] M. Palombo, A. Gabrielli, S. De Santis, C. Cametti, G. Ruocco, and S. Capuani, J. Chem. Phys. **135**, 034504 (2011).

[6] M. Palombo, A. Gabrielli, V. D. P. Servedio, G. Ruocco, and S. Capuani, Sci. Rep. **3**, 2631 (2013).

[7] P. Brault, C. Josserand, J.-M. Bauchire, A. Caillard, C. Charles, and R. W. Boswell, Phys. Rev. Lett. **102**, 045901 (2009).

[8] S. Wu, P. Brault, C. Wang, and B. Courtois, Appl. Surf. Sci. **266**, 400 (2013).

[9] S. Wu, P. Brault, C. Wang, and T. Sauvage, Physica A **390**, 2112 (2011).

[10] M. J. Saxton, Biophys. J. **103**, 2411 (2012).

[11] B. Bijeljic, A. Raeini, P. Mostaghimi, and M. J. Blunt, Phys. Rev. E **87**, 013011 (2013).

[12] P. de Anna, T. Le Borgne, M. Dentz, A. M. Tartakovsky, D. Bolster, and P. Davy, Phys. Rev. Lett. **110**, 184502 (2013).

[13] J. D. Moore, J. C. Palmer, Y.-C. Liu, T. J. Roussel, J. K. Brennan, and K. E. Gubbins, Appl. Surf. Sci. **256**, 5131 (2010).

[14] D. Roubinet, J.-R. de Dreuzy, and D. M. Tartakovsky, Comput. Geosci. **50**, 52 (2013).

[15] M. Sahimi, Phys. Rev. E **85**, 016316 (2012).

[16] L. Vasilyev, A. Raoof, and J. M. Nordbotten, Transp. Porous Med. **95**, 447 (2012).

[17] S. P. Neuman and D. M. Tartakovsky, Adv. Water Resour. **32**, 670 (2009).

[18] Y. Wang, Phys. Rev. E **87**, 032144 (2013).

[19] R. Metzler and J. Klafter, Phys. Rep. **339**, 1 (2000).

[20] E. K. Lenzi, H. V. Ribeiro, J. Martins, M. K. Lenzi, G. G. Lenzi, and S. Specchia, Chem. Eng. J. **172**, 1083 (2011).

[21] L. C. Malacarne, R. S. Mendes, I. T. Pedron, and E. K. Lenzi, Phys. Rev. E **63**, 030101(R) (2001).

[22] A. S. Balankin, B. Mena, C. L. Martínez-González, and D. M. Matamoros, Phys. Rev. E **86**, 052101 (2012).

[23] A. Giri, S. Tarafdar, P. Gouze, and T. Dutta, Geophys. J. Int. **192**, 1059 (2013).

[24] D. S. Novikov, E. Fieremans, J. H. Jensen, and J. A. Helpern, Nat. Phys. **7**, 508 (2011).

[25] N. Korabel and E. Barkai, Phys. Rev. Lett. **104**, 170603 (2010).

[26] F. Family and T. Vicsek, J. Phys. A **18**, L75 (1985).

[27] M. J. Vold, J. Coll. Sci. **14**, 168 (1959); J. Phys. Chem. **63**, 1608 (1959).

[28] F. Hivert, S. Nechaev, G. Oshanin, and O. Vasilyev, J. Stat. Phys. **126**, 243 (2007).

[29] E. Katzav and M. Schwartz, Phys. Rev. E **70**, 061608 (2004).

[30] F. D. A. Aarão Reis, Physica A **364**, 190 (2006).

[31] K. Khanin, S. Nechaev, G. Oshanin, A. Sobolevski, and O. Vasilyev, Phys. Rev. E **82**, 061107 (2010).

[32] C. A. Kennedy and W. C. Lennox, Stoch. Env. Res. Risk Assess. **15**, 325 (2001).

[33] S. Tarafdar and S. Roy, Physica B **254**, 28 (1998).

[34] D. Rodríguez-Pérez, J. L. Castillo, and J. C. Antoranz, Phys. Rev. E **72**, 021403 (2005).

[35] S. Sadhukhan, T. Dutta, and S. Tarafdar, J. Stat. Mech. (2007) P06006.

[36] A. Robledo, C. N. Grabill, S. M. Kuebler, A. Dutta, H. Heinrich, and A. Bhattacharya, Phys. Rev. E **83**, 051604 (2011).

[37] J. S. O. Filho, T. J. Oliveira, and J. A. Redinz, Physica A **392**, 2479 (2013).

[38] F. A. Silveira and F. D. A. Aarão Reis, Phys. Rev. E **75**, 061608 (2007).

[39] I. T. Pedron, R. S. Mendes, L. C. Malacarne, and E. K. Lenzi, Phys. Rev. E **65**, 041108 (2002).